Journal of the European Ceramic Society 22 (2002) 2799–2804

www.elsevier.com/locate/jeurceramsoc

Zirconia/stainless-steel continuous functionally graded material

S. López-Esteban, J.F. Bartolomé, C. Pecharromán, J.S. Moya*

Instituto de Ciencia de Materiales de Madrid (ICMM), Consejo Superior de Investigaciones Científicas (CSIC), Cantoblanco, 28049, Madrid, Spain

Received 18 October 2001; received in revised form 13 February 2002; accepted 24 February 2002

Abstract

A close to theoretical density zirconia/stainless steel continuous functionally graded material has been fabricated starting from coarse (≈20 μm) commercial metal powder by a wet processing method (pressure slip casting). The shape of the metal concentration profile has been characterized by image treatment. The dependence of the electrical properties of the material with the metal concentration presents a percolative behaviour with a metal-insulator transition, in addition to an increment of the capacity in the neighbourhood of a critical volume concentration, $f_c \approx 0.285$, approximately. Finally, the Vickers hardness vs metal concentration has been determined. Likewise, the results were compared with those obtained from composites with uniform metal concentration.

Keywords: Slip casting; Functionally graded materials; Mechanical properties; Electrical properties; ZrO_2/stainless-steel

1. Introduction

The functionally graded material (FGM) concept has been conceived as a material in which the composition and structure gradually change, resulting in a corresponding variation in the properties of the material, including mechanical, thermal and electrical.[1,2] This concept can be applied to various materials for structural uses, based on the integration of incompatible functions such as the refractoriness of ceramics and the toughness of metals, and for functional applications—the direct conversion of thermal energy to electric energy—as well as to produce multifunctional devices.[3] The fabrication process of FGMs is a quite complex task. In this sense, most published works deal with laminated samples that are formed by homogeneous layers of different compositions. On the contrary, continuous FGMs are scarcely reported. An extraordinary effort has been made in order to develop continuous FGMs in a wide range of systems and it has been attained in several works.[4–6] The unique properties of metal–ceramic materials in regions close to the percolation threshold makes them adequate for a wide variety of devices applicable to detect critical changes, such as electro-mechanical sensors, wearing-sensors, etc.[7]

We have chosen 3 mol% Y_2O_3-doped zirconia (3Y–TZP) as the candidate ceramic material, which has excellent thermal barrier properties, anti-corrosion and wear resistance. In this case, stainless steel has been chosen because of its enhanced corrosion resistance, high temperature oxidation resistance and strength. Its low cost is an attractive point facing industrial applications. Previous works about ZrO_2/stainless-steel FGM deal with layered materials[8–14] obtained either by powder metallurgy or by stacking tape cast layers. However, the absence of interfaces between layers should provide evident advantages, helping the thermal stress relaxation effect of the compositional gradation. Thus, in order to eliminate such interlayers, the aim of the current study was to obtain a continuous and dense ZrO_2/stainless steel FGM by controlling the rheology of the suspensions with the starting mixture of powders.

2. Experimental procedure

The following commercially available powders have been used as raw materials: (1) tetragonal zirconia polycrystals (Y–TZP 3 mol%; TZ–3YS, Tosol, Corp., Japan), with average particle size $d_{50} = 0.6 \pm 0.1$ μm; (2) stainless steel powders (Höganäs AB, Sweden), average particle

* Corresponding author. Tel./fax: +34-1-334-9083.
E-mail address: jsmoya@icmm.csic.es (J.S Moya).

0955-2219/02/$ - see front matter
PII: S0955-2219(02)00046-8

Table 1
Formulation of the suspensions with a relative proportion of metal (stainless steel) of 40 vol.% used in this study, and summary of experimental results. The viscosity measurements provided correspond to a shear rate of 500 s^{-1}

Sample	Solids loading (wt.%)	Deflocculant (wt.%)	Sedimentation	Microstructure	Viscosity (mPa s)
70-1	70	1	Segregation	Agglomerates	3
80-1	80	1	Gradual segregation	Graded	20
80-3	80	3	Homogeneous	Homogeneous	27

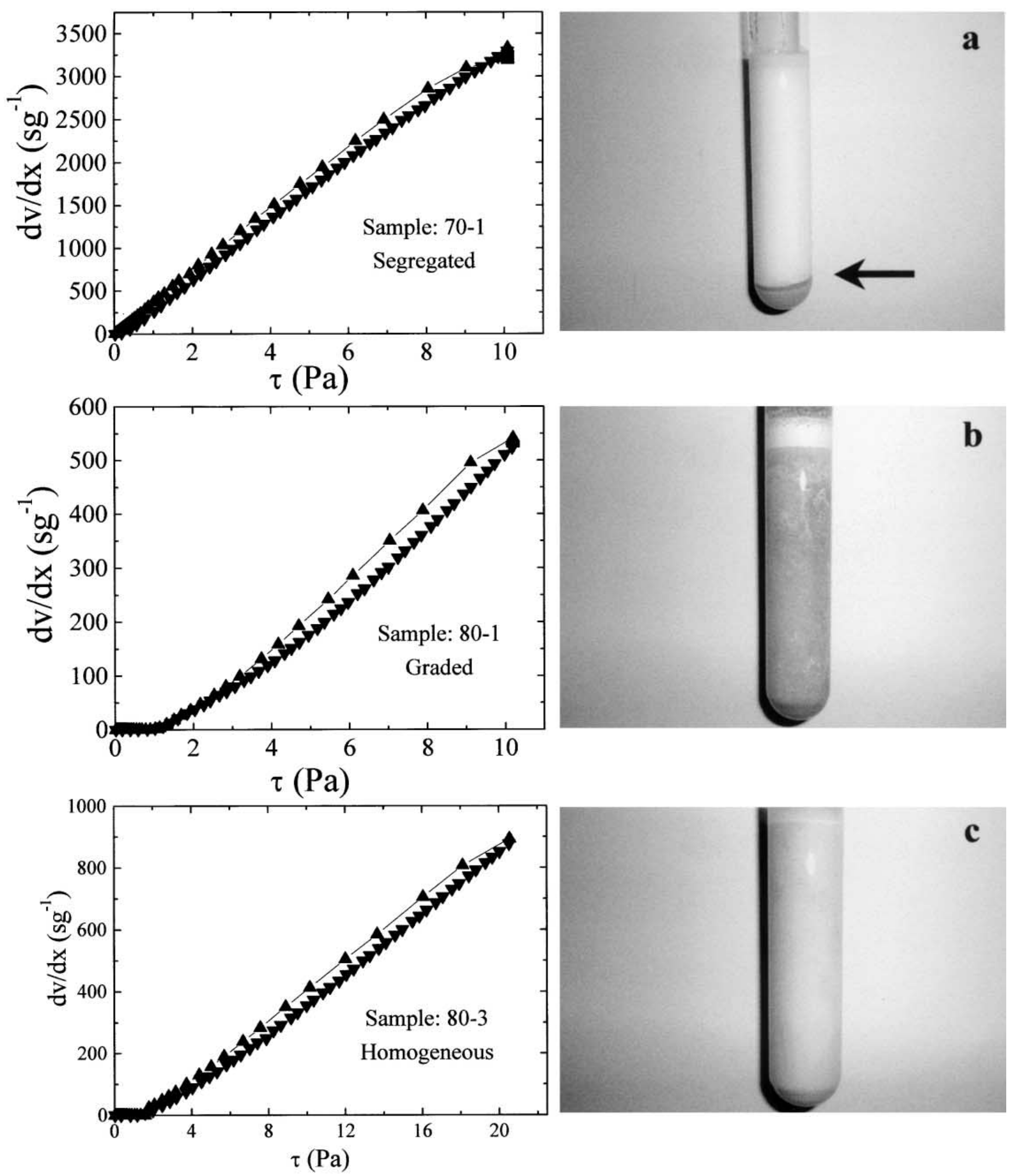

Fig. 1. Flow curves and sedimentation behaviour in glass tubes of the suspensions with 40 vol.% stainless steel: (a) 70 wt.% solid loading and 1 wt.% deflocculant, (b) 70 wt.% solid loading and 3 wt.% deflocculant, (c) 80 wt.% solid loading and 3 wt.% deflocculant.

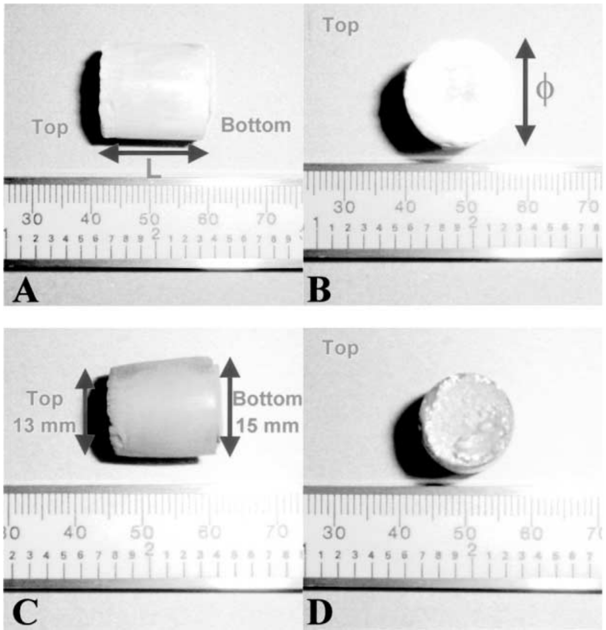

Fig. 2. Two views of the 3YTZP/stainless steel FGM obtained by slip casting. A and B correspond to the green body while C and D are referred to the sintered one.

diameter $d_{50} = 21.9 \pm 0.1$ μm and chemical analysis (wt.%): Cr (14.7%), Ni (10.5%), Mo (1.75%), Mn (0.11%).

Different ZrO_2/stainless steel suspensions of 70 and 80 wt.% solid content were prepared using distilled water as liquid media and a 1 and 3 wt.% addition of an alkali-free organic polyelectrolyte as surfactant with a relative proportion of metal of 40 vol.%. The mixtures were homogenized by milling with zirconia balls in polyethylene containers at 150 rpm for 24 h. Viscosity measurements have been performed using a rheometer Haake RS50 with a double gap cylinder sensor DG41 until a maximum value of 10 or 20 Pa depending on the suspension. The sedimentation behaviour of water-based slurries was studied at room temperature in glass test tubes for times up to 24 h. Several homogeneous samples with metal fraction 0.15, 0.20, 0.26 and 0.30 were obtained in order to obtain control measurements.

The FGM was obtained by slip casting in cylindrical PMMA tubes placed on plaster of Paris blocks. The pressure was kept constant at 0.2 MPa for 24 h. After drying, the sample was sintered in a tubular furnace in 90%Ar/10%H_2 atmosphere at 1350 °C for 2 h. The microstructures of fired specimen were studied on diamond polished surfaces down to 1 μm by scanning electron microscopy (Karl-Zeiss, DSM-950 model). The bulk densities were measured using the Archimedes, method.

The gradient was characterized along the longitudinal axis of the cross-section surface of the sintered sample polished down to 1 μm. The metal concentration in the FGM was determined by optical image treatment. This procedure was calibrated with micrographs obtained from monolithic composites of known and uniform metal concentration. The Vickers hardness profile, H_V, was measured using a Vickers diamond indenter (Leco 100-A). The applied load was 98 N in order to maximize the size of the indentations without generating cracks. The corresponding sizes were determined using an optical microscope (Leica DMRM). The variation of the dielectric constant and conductivity were determined by using a complex-impedance analyzer Solartron 1260.

3. Results and discussion

The results obtained from the sedimentation study of the suspensions as well as the microstructural aspects are summarized in Table 1. Fig. 1 shows the flow curves and sedimentation behaviour of suspensions prepared with 40 vol.% stainless steel. The suspension with 70 wt.% in solid content and 1 wt.% addition of surfactant suffered an important segregation of powders. This slurry displays a clear Newtonian behaviour (Fig. 1a). Fig. 1b corresponds to the suspension with a higher solid content (80%) and the same addition of surfactant (1 wt.%); the flow curve presents a clear plastic behaviour, slightly thixotropic; after sedimentation, the slurry presents a thin gradation. Finally, the suspension with 80 wt.% in solid content and 3 wt.% addition of surfactant was found to be homogeneous showing a plastic behaviour (Fig. 1c). The viscosity was measured at a shear rate of 500 s^{-1}. As can be seen in Table 1, such parameter increases with the solid loading and the deflocculant addition in such a way that it was necessary to increase the final shear stress to 20 Pa in suspension 1c to perform the test. Likewise, the sedimentation as well as the microstructure of the fired specimens point out that in order to obtain a FGM with controlled graded microstructure the most convenient suspension is the one shown in Fig. 1b.

The green body (Fig. 2A and B) displays a cylindrical shape of 20 mm length and 18 mm diameter. As can be observed in Fig. 2C and D, after sintering the sample suffered a differential shrinkage along the cylinder axis ranging from 28% at the top diameter to 17% at the bottom diameter. This is due to the increasing concentration of metallic particles in the cylindrical sample from top to bottom. The porosity of the fired cylinder was found to be less than 2 vol.%.

As can be observed in several optical micrographs of the cross-sectioned FGM (Fig. 3A–C) the metallic particles are homogeneously distributed into the ceramic matrix and there is no evidence of agglomerates. The final concentration profile (Fig. 3D) shows an increase in metal content until it reaches a maximum value of around 50 vol.% at about 0.3 L_0 (in Fig. 3A). Then, the steel content decreases monotonically (Fig. 3B and C) until 0 vol.% at $L = L_0$. A detail of the gradient is shown in Fig. 3E.

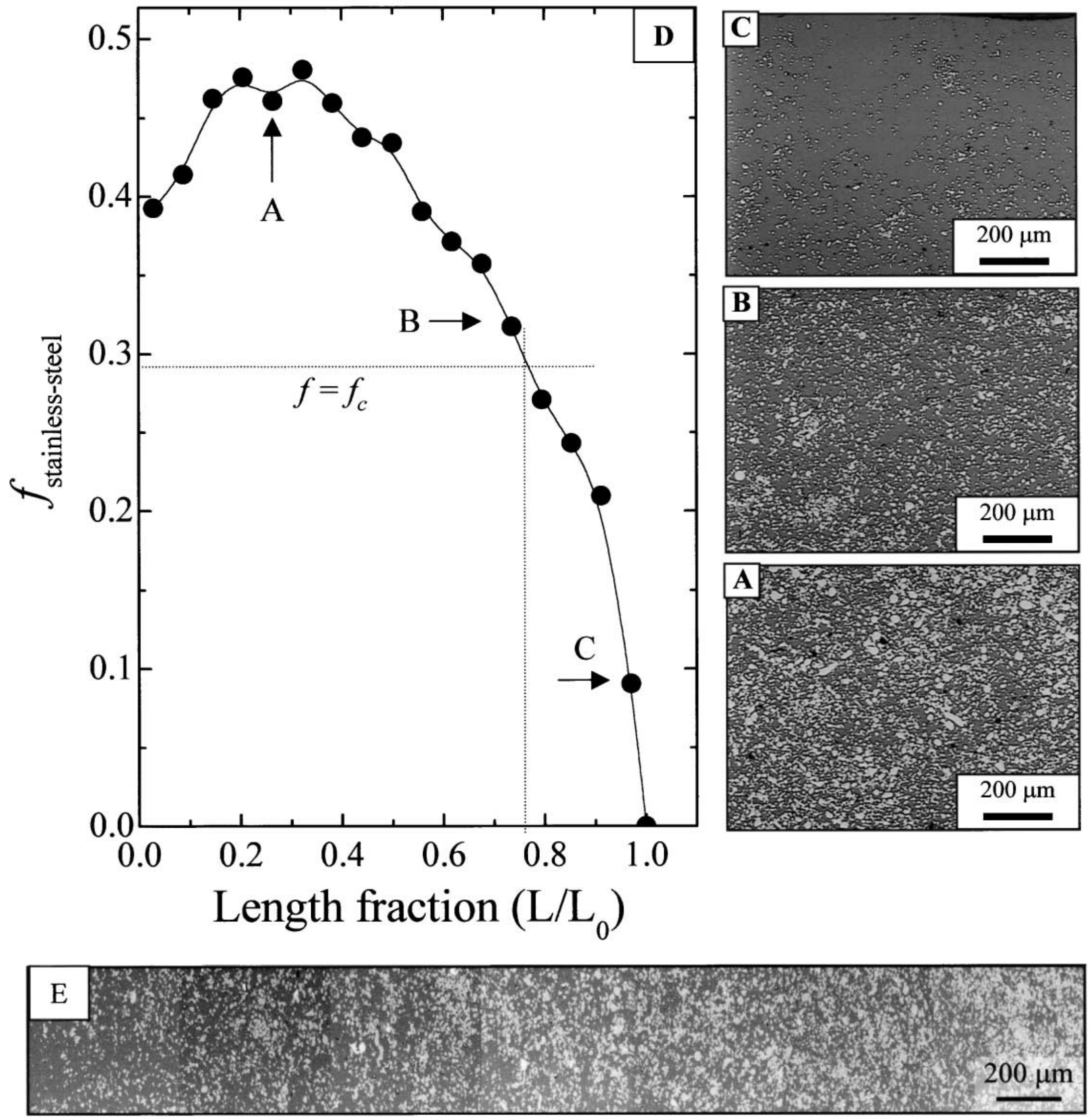

Fig. 3. Characterization of the FGM by image treatment. A, B and C: SEM micrographs showing the gradient at points located on Fig. 3D. D: plot of the filling factor of metal vs length fraction. E: detail of the gradient.

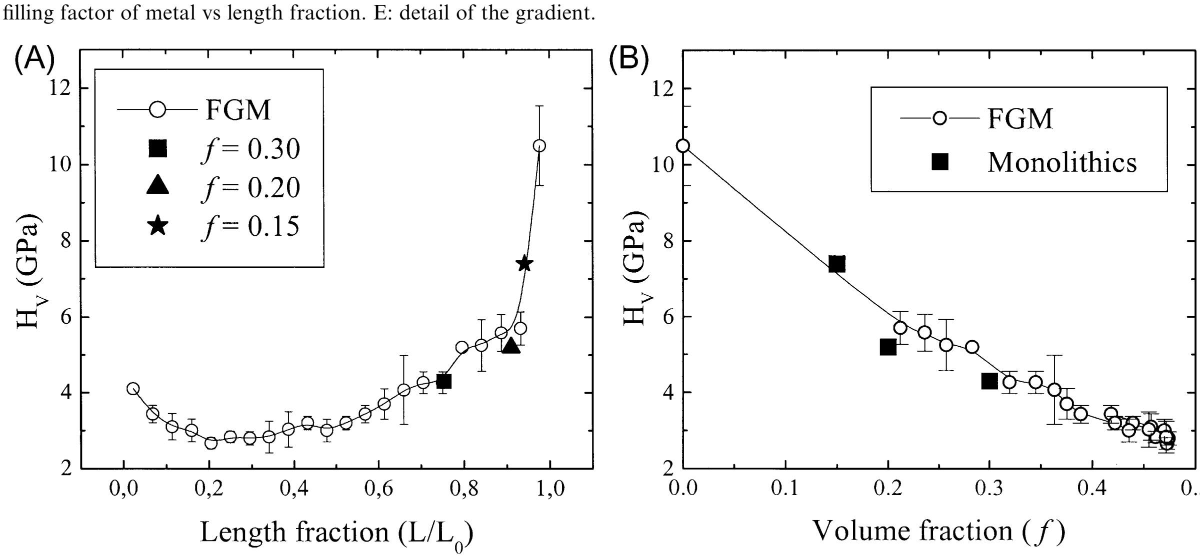

Fig. 4. Characterization of the gradient and comparison with the results obtained on composites: Vickers hardness profile vs length fraction (A) and vs metal volume fraction (B).

Once the slurry has been poured into the mould, a cake almost immediately forms at the bottom surface due to the fact that the coarser steel particles settle very fast at the beginning of the pressurized slip-casting operation. The initial suction carried out by the mould removes the liquid excess, maintaining the homogeneous situation. Thus, at the bottom surface, in contact with the mould ($L=0$) the metal volume fraction is 40 vol.%. The final shape of the profile depends on the combination of differential sedimentation velocity of the metal particles and ceramic particles and drying of the slurry. The rheological behaviour of this system has allowed obtaining a FGM with a metal particle size 20 times greater than that used in previous works.[4,5]

Fig. 4 shows the Vickers hardness profile on the FGM cross-section vs both the length fraction (L/L_0, Fig. 4A) and the metal fraction (f, Fig. 4B), as well as the results obtained from the monolithic composites prepared with different stainless steel content. Monolithic and continuous FGM present similar values of hardness. It monotonous and nearly linear reduces with steel concentration. As can be observed in Fig. 5A, the crack follows the zirconia/stainless steel interface. The crack propagates smoothly through the ceramic matrix and, on intercepting the metal particles, it follows the weak ZrO_2/stainless steel interface. Likewise, Fig. 5B shows the fracture surface as well as the intergranular fracture. There was no indication of plastic deformation of metal particles.

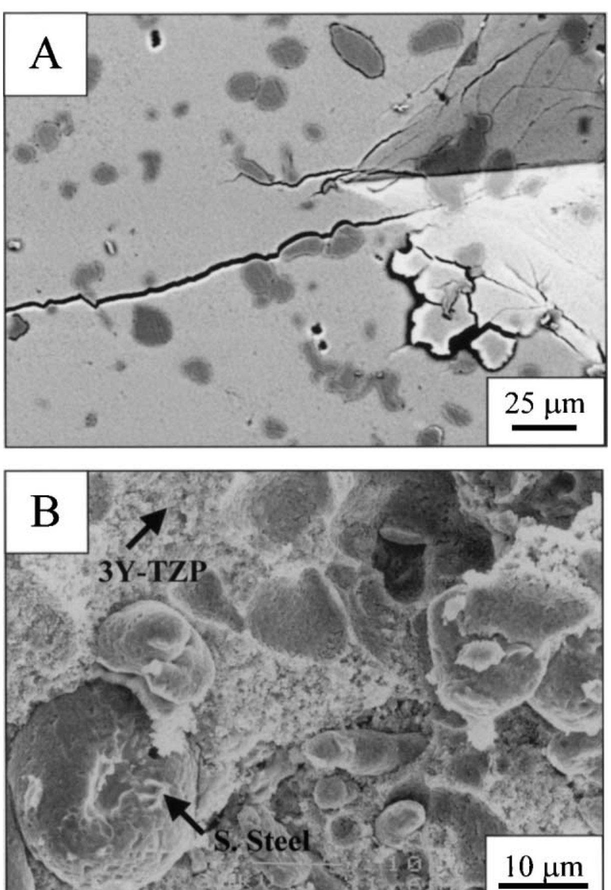

Fig. 5. (A) SEM micrograph illustrating the form of a crack initiated through a Vickers indentation; the lighter phase corresponds to zirconia and the darker phase is metal. (B) SEM micrograph of a fracture surface.

In continuous metal–ceramic FGM the metal concentration varies monotonously along one direction. Thus, there must be a part where the material abruptly changes from insulator to conductor. This point corresponds to the critical metal concentration or percolation threshold, f_c. The percolation threshold was determined on the polished FGM surface by 4-point conductance measurements (Fig. 6) and was found to be $f_c=0.28\pm 0.01$. This result agrees with the extrapolated value obtained from the fit of dielectric constant of monolithic samples with different metal content, according to the expression given by the general percolation theory:[15]

$$\langle \varepsilon \rangle = \varepsilon_m \left| \frac{f_c}{f_c - f} \right|^q \quad (1)$$

where ε_m is the dielectric constant of the matrix, f_c is the percolation threshold and f is the filling factor of the composite. The fit for the ZrO_2/stainless steel composites to this expression gives $q=0.84\pm0.06$ and the

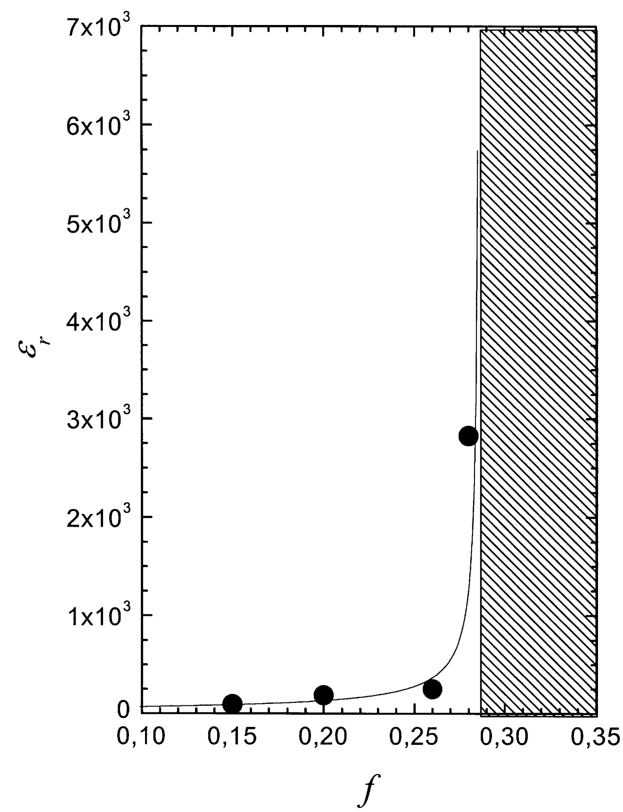

Fig. 6. Relative dielectric constant (ε_r) measured over monolithic samples vs filling factor (f) and curve fit. Shaded region corresponds to the conductor compositions on both monolithic samples and FGM.

extrapolated value for the percolation threshold $f_c = 0.285 \pm 0.015$, which agrees very well with the real value measured on the FGM.

4. Conclusions

A zirconia/stainless steel continuous FGM with density close to theoretical has been prepared by pressure slip casting. The gradient was characterized by image treatment, mechanical and electrical measurements and the results were corroborated with those obtained from composites with uniform metal concentration. The percolation threshold (metal/insulator transition) was found to be located at $f_c \approx 0.28$. These results have an important technological interest because of the nature of the metallic powder (stainless steel) and because of its coarse particle size (≈20 μm, commercial).

Acknowledgements

This work was supported by the Ministry of Science and Technology, Spain, under Project No. MAT2000–1354.

References

1. Krstic, D. V., On the fracture of brittle-matrix/ductile-particle composites. *Philos. Mag. A*, 1983, **48**, 695–708.
2. Hu, W., Guan, H., Sun, X., Li, S., Fukumoto, M. and Okane, I., Electrical and thermal conductivities of nickel–zirconia cermets. *J. Am. Ceram. Soc.*, 1998, **81**, 2209–2212.
3. Sajgalík, P. and Lencés, Z., ed., *Key Engineering Materials*. Trans. Tech. Publ. Ltd., Switzerland, 2000 (Vols. 175, 176).
4. Moya, J. S., Bartolomé, J. F., Diaz, M. and Requena, J., Mullite/molybdenum composites. *Composite Interfaces*, 1999, **6**, 325–342.
5. Tomsia, A. P., Saiz, A., Ishibashi, H., Diaz, M., Requena, J. and Moya, J. S., Powder processing of mullite/Mo functionally graded materials. *J. Eur. Ceram. Soc.*, 1998, **18**, 1365–1371.
6. Ishibashi, H., Tobimatsu, H., Matsumoto, T., Hayashi, K., Tomsia, A. P. and Saiz, E., Characterization of Mo–SiO_2 functionally graded materials. *Metallurgical and Materials Transactions A*, 2000, **31A**, 299–308.
7. Pecharromán, C. and Moya, J. S., Experimental evidence of a giant capacitance in insulator–conductor composites at the percolation threshold. *Adv. Mater.*, 2000, **12**, 294–297.
8. Omori, M., Sakai, H., Okubo, A. and Hirai, T., *Proceedings of the Third International Symposium on Structural and Functional Gradient Materials*. Presses Polytechniques et Universitaires Romandes, Lausanne, 1995 (p. 65).
9. Chen, Z., Ikeda, K., Murakami, T. and Takeda, T., Extrusion of metal–ceramic composite pipes. *J. Am. Ceram. Soc.*, 2000, **83**, 1081–1086.
10. Jung, Y.-G., Paik, U. and Choi, S. C., Influence of the particle size and phase type of zirconia on the fabrication and residual stress of zirconia/stainless steel 304. *J. Mater. Sci.*, 1999, **34**, 5407–5416.
11. Jung, Y.-G., Choi, S.-Ch., Oh, Ch.-S. and Paik, U.-G., Residual stress and thermal properties of zirconia/metal (nickel, stainless steel 304) functionally graded. *J. Mater. Sci.*, 1997, **32**, 3841–3850.
12. Yeo, J.-G., Jung, Y.-G. and Choi, S.-Ch., Design and microstructure of ZrO_2/SUS316 functionally graded materials by tape casting. *Mater. Lett.*, 1998, **37**, 304–311.
13. Yeo, J.-G., Jung, Y.-G. and Choi, S.-Ch., Zirconia–stainless steel functionally graded materials by tape casting. *J. Eur. Ceram. Soc.*, 1998, **18**, 1281–1285.
14. Kawasaki, A. and Watanabe, R., Fabrication of disk-shaped functionally gradient materials by hot pressing and their thermomechanical. In: *Functionally Gradient Materials, Ceramic Transactions,* vol. 34, ed. J.B. Holt, M. Koizumi, T. Hirai, and Z.A. Munir. The American Ceramic Society, pp. 157–164.
15. Efros, A. L. and Shklovskii, B. I., Critical behaviour of conductivity and dielectric constant near the metal–non metal transition threshold. *Phys. Stat. Sol. (B)*, 1976, **76**, 475–485.